The Simulated Sea: A Molecular Dynamics Study of Salt Ion Hydration and Interactions

Arin Khare

Abstract

Water makes life possible. Its unique structure leads to the formation of complex organizational patterns around various biomolecules such as DNA, RNA, and proteins, allowing it to mediate interactions between these bodies. Electrostatic charges are present on the surfaces of all of these molecules, and furthermore, the intracellular environment contains salt ions whose concentrations are tightly controlled to ensure biological signaling and function. Therefore, examining how water hydrates ions and mediates interactions between them is important to understanding processes of life. Here, we aim to answer the question: is the strength of association between salt ion pairs in water related to how strongly each ion is hydrated individually? Macroscopic experimental studies of salt solutions indicate that similarly-hydrated ions of opposite charges associate strongly with each other, a relationship captured by the volcano plot. To date, there exists no molecular equivalent to this relationship. In this study, we performed molecular dynamics simulations of 16 alkali-halides in water baths using the extended simple point charge model (SPC/E). Hydration free energies and ion-ion potentials of mean force were used to construct a molecular volcano plot, which revealed that the effective interaction strengths between salt ions are greater when the ions are hydrated similarly. This result is in agreement with previous experimental data, and has implications in biomolecular structure and function, drug design, downstream bioprocessing, and developing stable drug formulations. Future work may include extending the volcano plot to molecular ions prevalent in biological systems.

Introduction

It is generally understood that water mediates many of the interactions between DNA, RNA, and proteins. Existing studies focus primarily on hydrophobic interactions[1], but another part of the picture is related to the electrostatic charges that are present on the surfaces of biological macromolecules and in solution in the intracellular environment.

In 1969, Morris showed that the standard heat of solution of alkali-halides in water is related to their absolute heats of hydration using macroscopic experiments[2], creating what is known as the volcano plot, or the law of matching affinities. In 1997, Collins developed a theory of biological structure and function based on this observation that ions of similar sizes stick together in water[3]. However, these ideas are based upon assumptions which are fundamentally nanoscopic in nature, thus motivating the need for a molecular model of ion hydration and their water-mediated interactions.

Methods

Molecular Dynamics

Molecular dynamics simulations were conducted of 16 pairs of alkali-halides using the GROMACS software package[4]. Simulations of salt solutions were used to measure association strength, and simulations of individual ions were used to calculate hydration free energies.

All simulations were conducted in a bath of SPC/E[5] water in cubic boxes using periodic boundary conditions. Forces between atoms were calculated using the Lennard-Jones model for Van der Waals interactions and Lorentz-Berthelot combining rules. Electrostatic interactions were computed using the Particle Mesh Ewald algorithm. Forces were integrated using the leap-frog Verlet algorithm. Before each simulation, two steepest descent energy minimizations were run to obtain a stable starting configuration, first with flexible water and then with rigid water. Next, a 0.1 ns NVT equilibration was performed at 298.15K using the Nosé-Hoover thermostat, followed by a 1.0 ns NPT equilibration at 1 bar using the Parrinello-Rahman barostat. The production runs were performed in an NPT ensemble, and thus required both temperature and pressure coupling.

Ion	**σ (radius), nm**	**ε (well depth), kJ/mol**	**Mass, amu**	**Charge, e**
Na^+	0.2583	0.4184	23.000	+1
K^+	0.3331	0.4184	39.908	+1
Rb^+	0.3527	0.4184	85.468	+1
Cs^+	0.3883	0.4184	132.904	+1
F^-	0.3117	0.7531	19.000	-1
Cl^-	0.4401	0.4184	35.450	-1
Br^-	0.4623	0.4184	79.904	-1
I^-	0.5167	0.4184	126.900	-1

Table 1. The Dang ion parameters[6] were used in all molecular dynamics simulations.

Hydration Free Energy

Single ion simulations were performed in boxes with ~2.3 nm side lengths containing 391 water molecules over 10.0 ns at a 2.0 fs time step, saving configurations every 1.0 ps. For each ion, one simulation was performed in which the ion had no charge, and another in the natural charged state. The average electrostatic potential at the center of the ion due to the surrounding waters was calculated in both states, and these two values were used to compute the charging free energy of each ion. This value has been shown to make a dominant contribution to hydration free energy, so the effects of Van der Waals forces and cavity formation were omitted.

Hydration free energies were calculated using the methods devised by Hummer, Pratt, and Garcia[9]. This begins with the potential distribution theorem for free energy difference:

$$\Delta G = -\frac{1}{\beta} \ln \langle e^{-\beta \Delta U(\vec{x})} \rangle_{q_{sim}} \qquad (1)$$

Where β is the reciprocal of Boltzmann's constant multiplied by the temperature, and ΔU is the difference in potential energy between two systems (different charge states of the ion), if they are in the same configuration (coordinate locations of all atoms).

The potential energy difference can be quantified using the electrostatic potential at the center of the ion in the different charge states:

$$\Delta U(\vec{x}) = (q_{ion} - q_{sim})\phi \qquad (2)$$

Applying a cumulant expansion to equation 1, we can write that:

$$\Delta G = \sum_{n=0}^{\infty} \frac{C_{n,q_{sim}}(-\beta)^{n-1}}{n!}(q_{ion} - q_{sim})^n \qquad (3)$$

This is equivalent to the Taylor expansion of hydration free energy with respect to the charge of the ion and centered around the charge at which it was simulated. Therefore, the nth derivative of charging free energy at a given simulated charge state can be found using the nth cumulant of the electrostatic potential at the center of the ion (mean, variance, skewness, etc.). For the purposes of this study, only first cumulants, and thus first derivatives were calculated. This provides sufficiently accurate results, since the hydration free energy of ions has been shown to be roughly quadratic (describable using only two first derivatives) with respect to charge[7].

$$\left.\frac{\partial^n \Delta G}{\partial q_{ion}^n}\right|_{q_{ion}=q_{sim}} = C_{n,q_{sim}}(-\beta)^{n-1} \qquad (4)$$

Ion-hydrogen and ion-oxygen radial distribution functions were calculated using FORTRAN. The A-B radial distribution function $g_{A\text{-}B}(r)$ gives the density of atom B at a distance r from atom A relative to the bulk density of atom B. Multiplying the unnormalized radial distribution functions by the charges of the oxygen and hydrogen site of SPC/E water, respectively, and adding them together gives the radial charge density distribution from the center of the ion. Integrating this over the volume of the spherical shell represented by each r-value gives the electrostatic potential at the center of the ion.

$$\phi(R) = \int_0^R \frac{\rho_q(r)dV}{4\pi\epsilon_0 r} \qquad (5)$$

Where $\rho_q(r)$ is the charge density at a distance r from the ion center, and ϵ_0 is the permittivity of free space.

As the integral in equation 5 is computed, it takes into account a greater number of water molecules' contributions to the electrostatic potential. Beyond a certain distance, the ion no longer has any influence on the surrounding waters, so the integral of charge density should converge as charge density approaches zero. However, this proves not to be the case, due to the statistical fluctuations in the radial distribution function, as well as the contributions from periodic images. To correct this, we note that according to continuum electrostatics, water should form a sphere around the solute that is roughly equal and opposite in charge to the ion. Assuming that this is true at all distances from the ion, and that the "missing" charge is evenly distributed, a background charge correction term is added to the electrostatic potential calculation.

$$\phi_{bgd}(R) = \frac{3}{2}\frac{q_{bgd}}{R}\frac{1}{4\pi\epsilon_0} \qquad (6)$$

where:

$$q_{bgd}(R) = -(q_{ion} + q_{pol}(R))$$

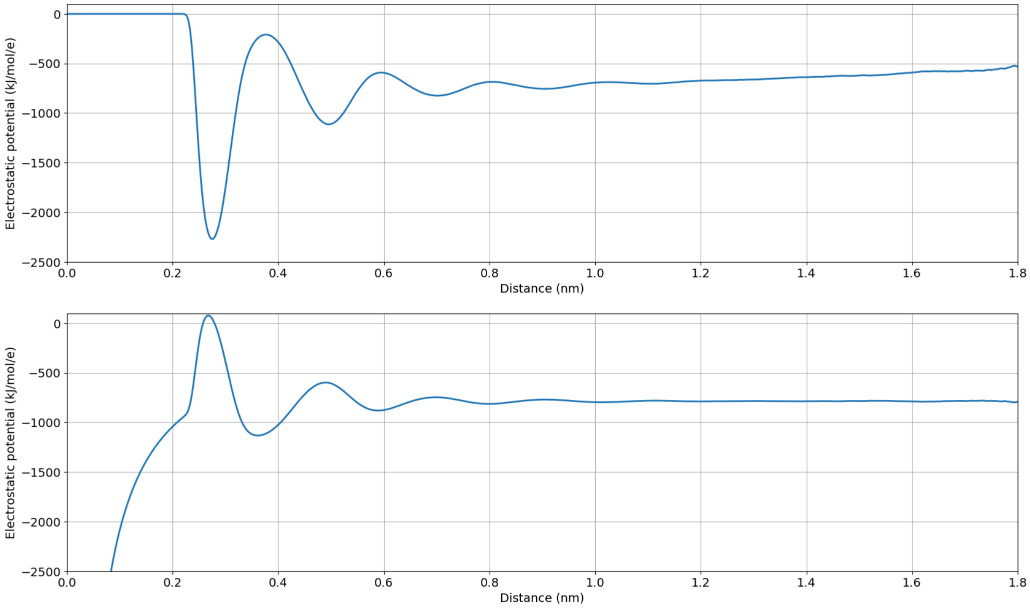

Figure 1. (Top) Electrostatic potential as a function of distance from the center of a charged Na^+ ion in water (equation 5). This integral does not converge. (Bottom) Electrostatic potential at the center of Na^+, with the background charge correction applied (equation 6).

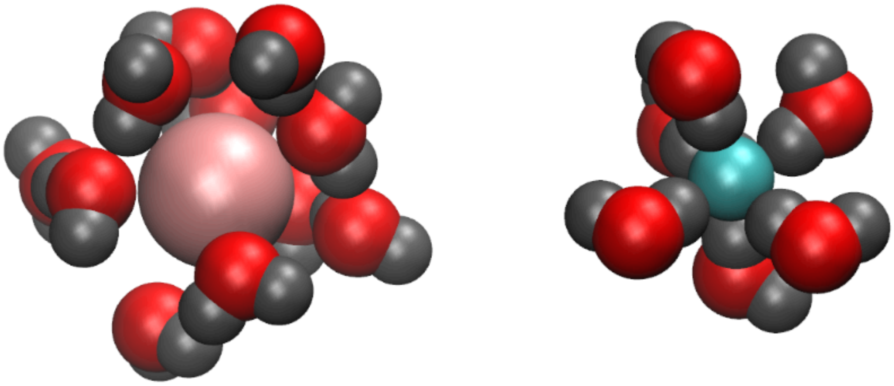

Figure 2. (Left) Hydration shell of Cs^+. As a large ion, Cs^+ is not strongly hydrated, as can be seen by the fact that its hydration waters have significant variation in their orientations. (Right) Hydration shell of F^-. As a small ion, F^- is strongly hydrated, as can be seen by the fact that all hydrogen atoms of its hydration waters are pointed directly at the ion center. Additionally, its hydration shell is significantly smaller than that of Cs^+.

Salt Ion Association Strength

16 simulations of 1M concentrated salt solutions were performed. 10 ion pairs were placed in a box with ~2.55 nm side length along with 528 water molecules. These were modeled over 20.0 ns at a 2.0 fs time step, saving configurations for analysis every 1.0 ps. From these simulations,

ion-ion association strength was obtained. A potential of mean force (PMF)[8] was calculated over the distance between the opposite charges, using the ion-ion radial distribution function. In all cases, the first two minima of the PMF were identified to correspond to the contact (associated) and solvent-separated (non-associated) states. The difference in height between these PMF values was used to indicate ion-ion association, and is represented by ΔW.

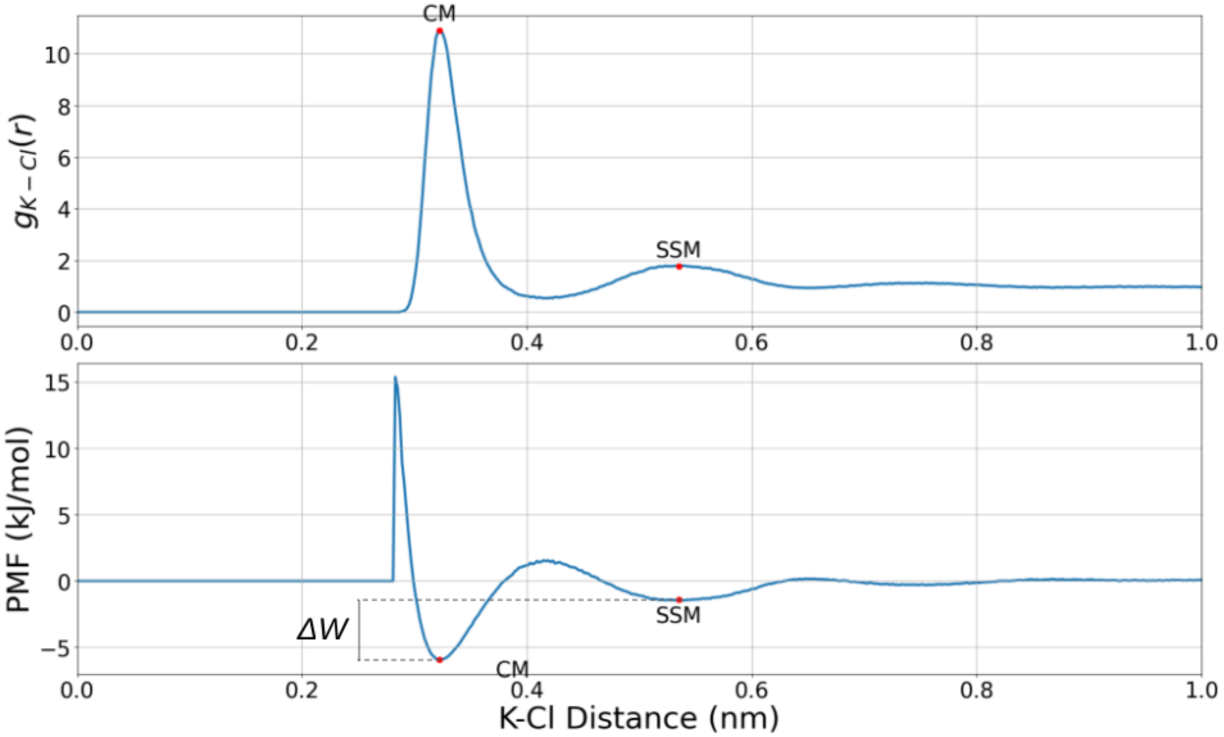

Figure 3. (Top) KCl ion-ion radial distribution function. (Bottom) Potential of mean force over K-Cl distance. (-kTln[g(r)]). The shape of both distributions is a result of the structures formed by waters around the ion.

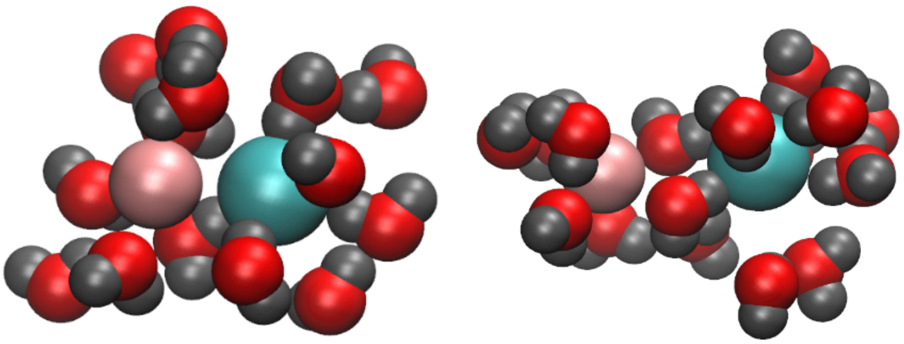

Figure 4. (Left) A contact pair of KCl. (Right) KCl in the solvent-separated state.

Results

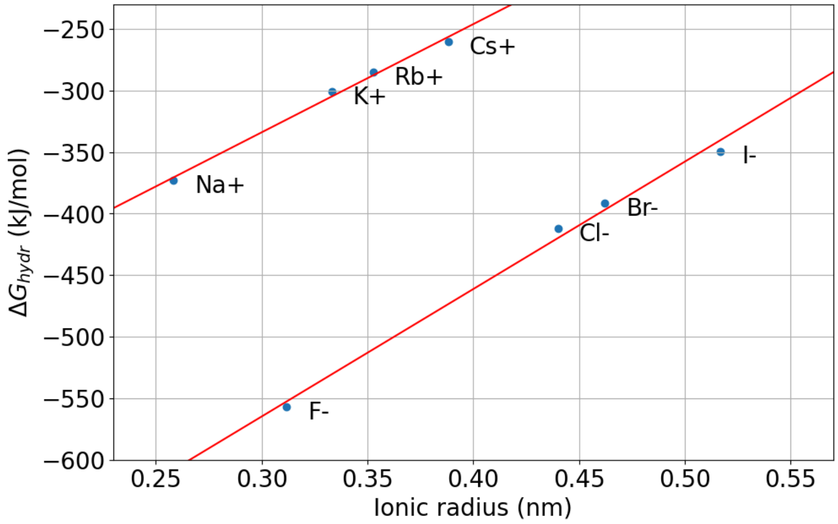

Figure 5. Hydration free energy as a function of ionic radius.

In accordance with previous results, hydration free energy was found to be more negative for anions than for cations of the same ionic radius[7]. Additionally, it was found to have a strong linear relationship with ionic radius for both cations and anions, another known relationship[3].

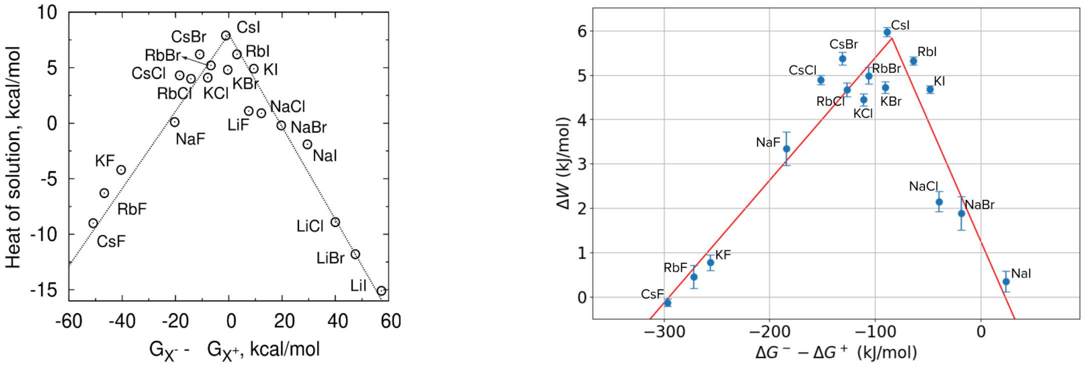

Figure 6. (Left) Standard heat of solution as a function of the difference in absolute heats of hydration (anion minus cation). Data reproduced from Morris, 1968[2]. (Right) The molecular volcano plot.

To construct the molecular volcano plot, *ΔW* values (as defined in the methods section, and illustrated in figure 3) were plotted over the difference in hydration free energy (anion minus cation). In comparison to Morris' results, it is worth noting not only the persistence of the volcano relationship, but also the agreement of the relative locations of each of the alkali-halides. Linear regressions on each side of the molecular volcano (including CsI in both datasets) provide R^2 values of 0.933 to the left of the peak and 0.888 to the right.

Discussion

This result provides support for the model of biological organization developed by Collins, who posited that the relative concentrations of the major intracellular ions are regulated in order to prevent the formation of contact pairs between similarly-sized ions of opposite charges. A future study applying these procedures to molecular ions may also provide support for Collins' idea that sodium-potassium pumps were formed in order to prevent Na^+ from binding with nucleic acid phosphate oxyanions.

A model of the effective strength of ion-ion interactions in water can be used to engineer biopharmaceuticals with particular binding sites. These findings can also be used to determine concentrations of ionic solutions in which to dissolve proteins in order to prevent precipitation. Additionally, it can be used to design ligands for protein chromatography used in downstream bioprocessing. Lastly, an understanding of water-mediated ion interactions could have applications in the field of protein crystallography.

One limitation of this study was that the calculation of charging free energy only took into account the average electrostatic potential at the center of the ion in the charged and uncharged states. These provide the first derivatives of charging free energy, and thus assumes that it is perfectly quadratic when used to calculate its value. While this has been found to be roughly correct in previous studies, information about second derivatives will undoubtedly lead to greater accuracy. The second derivative of charging free energy is equal to the variance of the electrostatic potential, which cannot be obtained from the radial distribution function and background charge correction. This would require an implementation of the Ewald summation.

Lithium was omitted from this project because a sufficient number of configurations in both the contact and solvent-separated states could not be observed in order to measure association strength with a reasonable level of precision. This may be remedied by applying non-Boltzmann sampling methods such as umbrella sampling.

Conclusions

In this paper, we present the first ever molecular equivalent to the volcano plot, showing that the effective strength of ion-ion interactions between alkali-halides in water is dependent on the hydration of each ion individually. Association strength was measured using the difference between the contact and solvent-separated minima in the potential of mean force over the distance between the two ions, and hydration free energies were calculated by simulating ions in charged and uncharged states. Our findings have various pharmaceutical applications, and enable further study of the role of water-mediated interactions between ions in biological systems.

Acknowledgements

I thank Dr. Shekhar Garde (mentor) for his guidance, and Riddhesh Patil (graduate collaborator) for aiding my understanding of the concepts underlying this project. I also thank my teacher sponsor, Mrs. Laura Favata.

References

[1] Rego, N. B., Xi, E., & Patel, A. J. (2019). Protein hydration waters are susceptible to unfavorable perturbations. *Journal of the American Chemical Society*, *141*(5), 2080-2086. https://doi.org/10.1021/jacs.8b11448

[2] Morris, D.F.C. (1968). Ionic radii and enthalpies of hydration of ions. In: Structure and Bonding. Structure and Bonding, vol 4. Springer, Berlin, Heidelberg. https://doi.org/10.1007/BFb0119185

[3] Collins, K. (1997). Charge density-dependent strength of hydration and biological structure. *Biophysical Journal*, *72*(1), 65-76. https://doi.org/10.1016/s0006-3495(97)78647-8

[4] Abraham, M. J., Murtola, T., Schulz, R., Páll, S., Smith, J. C., Hess, B., & Lindahl, E. (2015). GROMACS: High performance molecular simulations through multi-level parallelism from laptops to supercomputers. *SoftwareX*, *1-2*, 19-25. https://doi.org/10.1016/j.softx.2015.06.001

[5] Berendsen, H. J. C., Grigera, J. R., & Straatsma, T. P. (1987). The Missing Term in Effective Pair Potentials. *Journal of Physical Chemistry*, *91*, 6269-6271. https://doi.org/10.1021/j100308a038

[6] Koneshan, S., Rasaiah, J. C., Lynden-Bell, R. M., & Lee, S. H. (1998). Solvent Structure, Dynamics, and Ion Mobility in Aqueous Solutions at 25 °C. *The Journal of Physical Chemistry B*, *102*(21), 4193-4204. https://doi.org/10.1021/jp980642x

[7] Rajamani, S., Ghosh, T., & Garde, S. (2004). Size dependent ion hydration, its asymmetry, and convergence to macroscopic behavior. *The Journal of Chemical Physics*, *120*(9), 4457-4466. https://doi.org/10.1063/1.1644536

[8] Luksic, M., Fennell, C. J., & Dill, K. A. (2014). Using Interpolation for Fast and Accurate Calculation of Ion−Ion Interactions. Journal of Physical Chemistry B, 118, 8017-8025. https://doi.org/10.1021/jp501141j

[9] Humphrey, W., Dalke, A., & Schulten, K. (1996). VMD: Visual molecular dynamics. *Journal of Molecular Graphics*, *14*(1), 33-38. https://doi.org/10.1016/0263-7855(96)00018-5